



# Reciprocating Sliding Wear of Cu, Cu-SiC Functionally Graded Coating on Electrical Contact

Swastika Banthia, Mohammad Amid, Srijan Sengupta, Siddhartha Das, and Karabi Das

(Submitted September 27, 2019; in revised form May 13, 2020; published online June 13, 2020)

The present work evaluates the coefficient of friction (CoF), electrical resistivity, and electrical contact resistance (ECR) of the electrodeposited single-layered Cu-SiC nanocomposite coating and five-layered Cu, Cu-SiC functionally graded coating (FGC). Both the coatings have a similar thickness (60  $\mu\text{m}$ ) and same composition at the top surface (7 vol.% reinforced SiC nanoparticles), while the FGC has a gradient of composition and microstructure throughout the thickness. The Cu, Cu-SiC FGC has two layers of Cu-SiC with a decrement in the content of SiC nanoparticles from 7 to 2 vol.% followed by three Cu layers with an increasing crystallite size towards the substrate. The electrical resistivity of the Cu, Cu-SiC FGC is measured by the four-wire resistance measurement method and the value is observed to be 50% less than the conventional nanocomposite coating. A linear reciprocating sliding wear test is carried out at 2, 5 and 8 N load at a constant frequency and stroke length of 10 Hz and 2 mm, respectively. The monitored value of CoF is significantly less for the Cu, Cu-SiC FGC than the single-layered coating at 2 and 5 N loads and is nearly equal at 8 N load. It is observed that before wear, the ECR values of both the coatings are higher than the uncoated Cu and after wear the ECR value of Cu, Cu-SiC FGC is the lowest.

**Keywords** coefficient of friction, electrodeposition, electrical contact resistance, electrical resistivity, functionally graded coating

## 1. Introduction

The sliding electrical contact is an arrangement of similar or dissimilar materials where one of the contacts is stationary with respect to another. They are designed to have low electrical contact resistance (ECR) and low coefficient of friction (CoF) under contact forces with wear-resistant properties. The performance of any electrical contact material is governed by its surface, which has microscopic unevenness where the peaks are called asperities. When the electrical contacts are in closed condition, the real area of contact is at the sites of asperities, which are distributed across the apparent area of contact (Ref 1). The electrical contact materials require stable contact resistance in compact-complex spaces and prevention from unavoidable vibrations resulting in an oscillatory motion, which is known as fretting action (Ref 2-4). Under applied load conditions, the contact pressure at the real area of contact is

high and the fretting action results in surface wear, called fretting wear (Ref 5, 6). It is reported that the transition from fretting to sliding wear takes place at high amplitude, material removal, and at a constant wear factor (Ref 7).

Cu is long being used as a cost-effective electrical contact material with good formability, and high electrical and thermal conductivity. However, its performance in pure form is limited because of the low ultimate tensile strength and low yield strength, resulting in inferior tribological properties. The Copper Development Association has reported the physical and electrical properties of the most common electrical contacts used in some particular device (Ref 8). In general, sliding electrical contacts undergo excessive mechanical wear due to friction and sticking or cold welding at the asperities, which increase the ECR (Ref 9). There is a requirement of nanocomposite coating on the commercially available electrical contact material (Ref 10).

SiC is used as reinforcement in the Cu matrix composite to improve the mechanical and wear properties (Ref 11-13). Bindal et al. (Ref 14) have reported that the hardness of pure Cu increases with the addition of 3 wt.% of SiC, but the electrical conductivity reduces from 91.7 to 66.4% International Annealed Copper Standard (IACS). According to Guo et al. (Ref 15), a Cu/SiC functionally graded material (FGM) provides the required surface conductivity at Cu-rich end and graded structure is beneficial for low surface ECR. It is reported by Rahvard et al. (Ref 16) that for a Cu/NbC graded composite material, the increase in the value of electrical conductivity is two times than that of the traditional composite with the same mechanical and tribological properties. Raheem and Ali (Ref 17) have reported that five-layered Cu-Al<sub>2</sub>O<sub>3</sub> FGM can eliminate the microscopic interface and provides improved wear resistance for electrical contact application. Thus, there is a motivation to synthesize a FGM or a functionally graded nanocomposite coating on any conducting surface as a potential and novel electrical contact material.

**Swastika Banthia**, School of Nanoscience and Technology, Indian Institute of Technology Kharagpur, Kharagpur 721302, India; **Mohammad Amid**, Department of Metallurgical and Materials Engineering, Indian Institute of Technology Kharagpur, Kharagpur 721302, India; **Srijan Sengupta**, Department of Metallurgical and Materials Engineering, Indian Institute of Technology Jodhpur, Jodhpur, India; and **Siddhartha Das** and **Karabi Das**, School of Nanoscience and Technology, Indian Institute of Technology Kharagpur, Kharagpur 721302, India; and Department of Metallurgical and Materials Engineering, Indian Institute of Technology Kharagpur, Kharagpur 721302, India. Contact e-mails: karabi@metal.iitkgp.ernet.in and karabi@metal.iitkgp.ac.in.

Electrodeposition is a well-established technique to tailor the surface properties of an electrical contact material by changing the parameters (Ref 18, 19). The electrodeposited coatings on the surface of a conductive material can have a varying number of layers, thickness, morphology, and crystal shape (Ref 20–22). The incorporation of wear-resistant SiC nanoparticles in the Cu matrix is reported to provide resistance against sliding wear in the unlubricated conditions (Ref 23). However, the nanocomposite coatings are rough, possess high CoF and restrict the current flow to pass through a certain, limited number of points and increase the contact resistance (Ref 24). The high residual stress in the nanocomposite coatings is also undesirable for the electrical contact application (Ref 25). These properties can be improved by making the surface smooth and the electrodeposited FGC is reported to be highly efficient in sliding-wear-resistant application (Ref 26, 27). In our recent publication, electrodeposited Cu, Cu-SiC functionally graded coating (FGC) on annealed Cu substrate is reported to serve as a prospective electrical contact material for large scale industrial application (Ref 28). This paper focuses on the analyses of the CoF during the reciprocating sliding wear under constant load of 2, 5, and 8 N and evaluates the electrical properties of single-layered Cu-SiC nanocomposite coating and Cu, Cu-SiC FGC. This work highlights five-layered functionally graded coating (FGC), which has improved physical property (e.g., surface roughness and residual stress) with high hardness when compared to single-layered metallic and nanocomposite coatings (Ref 28). In the current work, the wear-resistant property of Cu, Cu-SiC FGC coating is evaluated and further, electrical properties are investigated before and after wear conditions. It is reported that electrodeposited Ni-based FG coating with a variation of microstructure or amount of reinforced phase along the thickness, which has improved wear and corrosion properties as compared to the single-layered coating (Ref 29–31,32). However, to the best of our knowledge, the suitability of such electrodeposited Cu, Cu-SiC FGC on Cu based electrical contact for protection against reciprocating sliding wear is not reported yet. Our work focuses on the interdisciplinary research which includes tailoring the surface related properties by optimizing the synthesis parameters of electrodeposition of Cu based coating for wear-resistant electrical contact applications.

## 2. Experimental Methods and Materials

A Cu block of area 4 cm<sup>2</sup> and 3 mm height was annealed at 400°C for 1 h and then air-cooled. In order to use it as a sample for electrodeposition, it was polished as per the protocol described in our previous publication (Ref 28). The details about the substrate and bath preparation (plating bath1 and 2), and electrodeposition parameters were described in our earlier publication (Ref 28). For the electrodeposition of Cu coating, an aqueous acidic copper sulfate bath (plating bath1) was prepared by using 0.8 M solution of CuSO<sub>4</sub>·5H<sub>2</sub>O (Loba Chemie, ≥ 98%) and 1 M sulfuric acid. The pH of the plating bath1 was adjusted to be less than 1 (0.12 + 0.02) at 23.7°C.

For the electrodeposition of 60-μm-thick, Cu-SiC nanocomposite coating with 7 vol.% of uniformly dispersed SiC nanoparticles (Fig. 1a), a plating bath2 was prepared by adding 1 mM of cationic N-Cetyl-N,N,N trimethyl ammonium bro-

mid (CTAB, SRL, 99%) surfactant and 10 g/L of SiC nanopowder (Alfa Aesar, β-phase) to plating bath1. From the plating bath2, a 60 μm thick, Cu-SiC nanocomposite coating with 7 vol.% of uniformly dispersed SiC nanoparticles was synthesized. A constant cathodic current density (CCD) of 200 mA/cm<sup>2</sup> and an anodic current density (ACD) of 66 mA/cm<sup>2</sup> was supplied for 50 ms each, followed by a relaxation time period of 50 ms after every current waveform. The plating bath2 was agitated at 450 rpm in order to uniformly disperse SiC nanoparticles in the Cu matrix during the deposition.

From plating bath1, the first three layers of Cu coating were deposited by increasing the CCD (50, 100, and 200 mA/cm<sup>2</sup>), while the ACD was kept one-third of the CCD. It was followed by deposition of two layers of Cu-SiC nanocomposite coating by introduction of plating bath agitation (350 and 450 rpm) at CCD and ACD of 200 and 66 mA/cm<sup>2</sup>, respectively. This resulted in a three layered Cu with decreasing crystallite size followed by two layers of Cu-SiC with increasing amount of SiC from 2 to 7 vol.% along the thickness of the coating. The five-layered (each 12 μm thick) Cu, Cu-SiC FGC consists of three layers of Cu coating and two layers of Cu-SiC nanocomposite coating (Fig. 1b).

The Ducom linear reciprocating tribometer was used to perform the reciprocating wear where, the E-52100 hardened steel (grade G24, ~ 8.5 GPa) ball of 6 mm diameter was used as a sliding counter material. The image of the equipment is shown in Fig. 2(a). The reciprocating sliding wear test was conducted for 6000 cycles at 25 ± 1°C under normal loads of 2, 5 and 8 N and with a periodic displacement of 2 mm and frequency of 10 Hz. The CoF was continuously monitored with the number of cycles. The test was conducted according to ASTM international standards (Ref 33). The volume loss in each sample was calculated from the dimensions of wear scar, which were obtained by using the non-contact mode of 3D optical surface profilometer (Contour GT, Bruker, Germany). The measurement of wear scar length, width and depth values was done thrice with three set of samples and the average value was used to calculate the volume loss.

The microstructural characterization and elemental mapping of the electrodeposited coatings were carried out using field emission scanning electron microscope (FESEM (Merlin, Carl Zeiss Microscope GmbH, Germany) equipped with an energy-dispersive x-ray spectrometer at an operating voltage of 20 kV.

The ECR measurement was made by using a D.C. two-wire circuit at room temperature in accordance with the ASTM standard test methods for measuring contact resistance of electrical connections (Static Contacts) (Ref 34). A setup was developed in which the ECR of the annealed, uncoated, and coated samples was measured using the sample holder, where two cube-shaped samples touch each other as illustrated in Fig. 2(b). When subjected to a force 'F', the samples were pressed against flat Cu surface (surface roughness of 0.1 μm), which was held in a fixed position and the ECR was measured at 100 mA.

The electrical resistivity of the electrodeposited coatings was measured by Keithley 2812 nano voltmeter and Keithley 2400 sourcemeter. The four-wire resistance measurement setup was developed (Fig. 2c). In this setup, there was a spacing of 0.2 cm between each gold-plated wire. A current of 0.2 mA was passed through the current probe by using a source meter and the voltage drop between the two middle probes was recorded by using a highly precise nanovoltmeter. Typical size of the samples used in this measurement was 6 cm × 1 cm ×

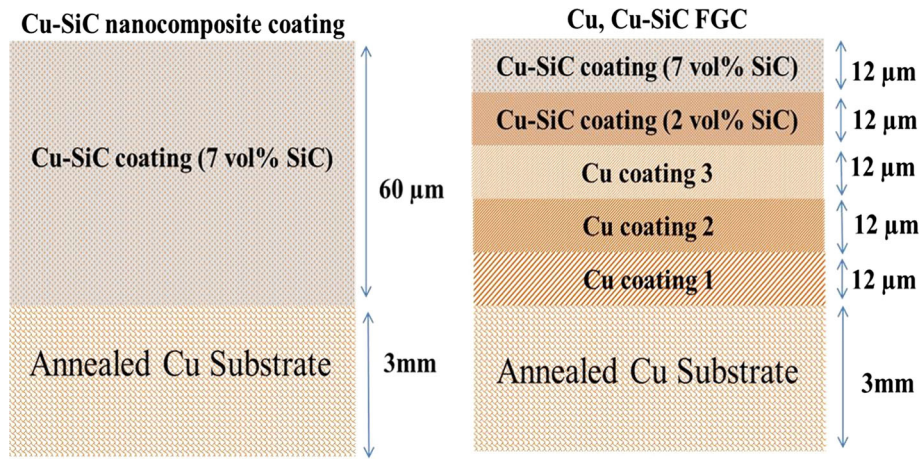


Fig. 1 Schematic representation of single-layered Cu-SiC nanocomposite coating and Cu, Cu-SiC FGC

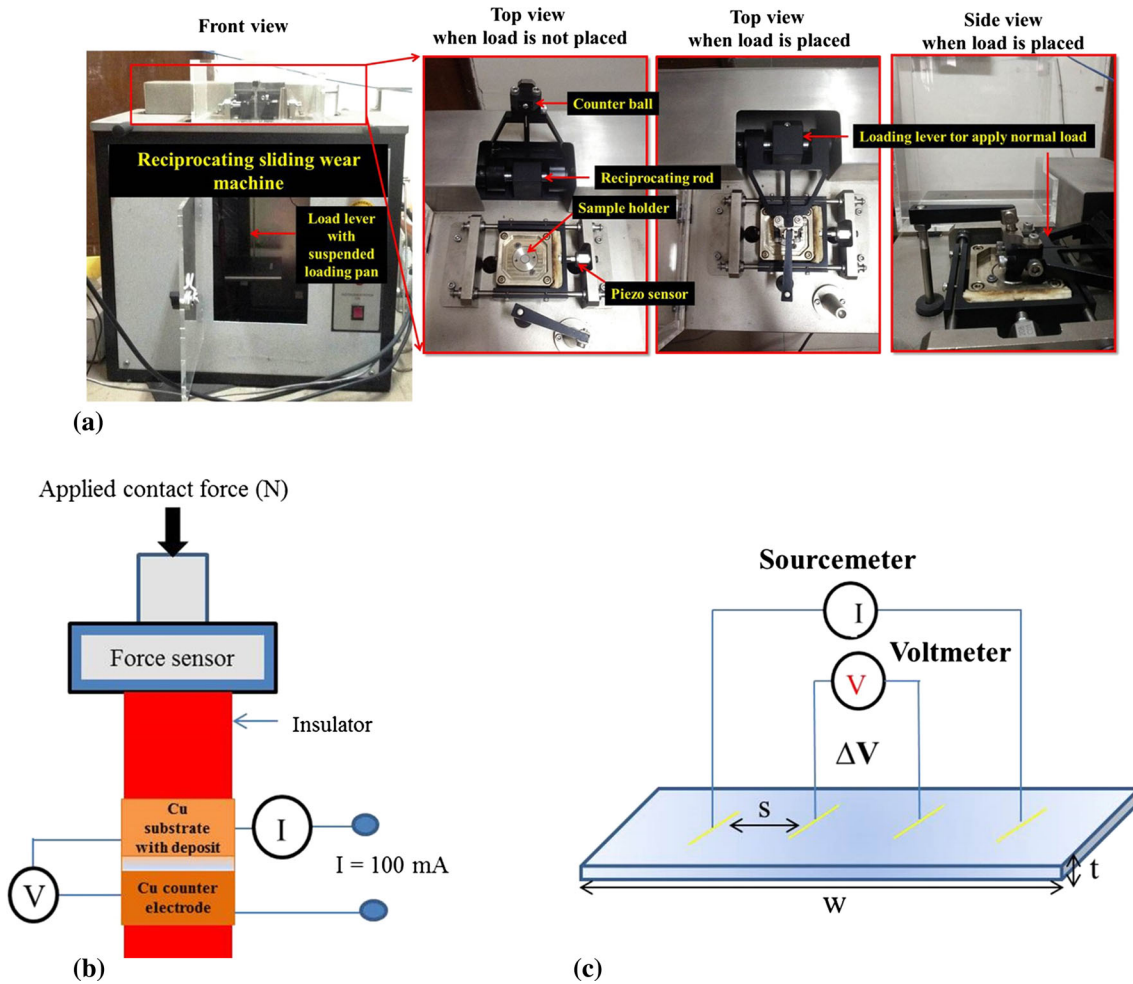


Fig. 2 (a) Reciprocating wear machine used in this investigation, (b) A schematic presentation of the contact resistance measurement setup (Ref 34) and (c) A schematic representation of the electrical resistivity setup

60  $\mu\text{m}$ . In this study, the sample's electrical resistance ( $R$ ) was calculated by dividing the voltage difference between the inner probes ( $\Delta V$ ) with current ( $I$ ) passing through the outer probes. The resistivity ( $\rho$ ) value was calculated by taking a product of

thickness ( $t$ ) and width of the sample ( $w$ ) with  $R$ , which is divided by probe spacing ( $s$ ). The measurement of sample's  $R$  and  $\rho$  value was done thrice with three set of samples and average value was reported.

### 3. Results and Discussion

Figure 3 shows the variation of CoF with the number of cycles at 2, 5 and 8 N loads for the annealed, uncoated Cu. An annealed Cu is soft with large grain size and readily oxidizes in air. It is observed from Fig. 3(a) that the CoF is initially low because the contact is between the counter hardened steel ball and the oxidized Cu surface, which has low shear strength and lubricating nature. With increase in cycles, the CoF increases because the oxide film is partially removed from the Cu surface. The metallic contact takes place between the Cu surface and counter steel ball, which increases the real area of contact and hence, the CoF increases. This period can be defined as 'run in time' marked as region I (Fig. 3(a-c)). After the 'run in time,' the CoF increases suddenly and this period is defined as 'transition period' (Region II) as shown in Fig. 3(a-c). The oxide layer is completely removed from the surface and metallic Cu surface is in contact with the counter hardened steel ball. With further increase in the number of cycles, the wear debris starts forming and results in an increase in the abrasive friction. However, at the same time, the real area of contact decreases, which leads to the decrement in the adhesive friction. Both seems to nullify each other and results in constant CoF with slight serrations. This period is defined as 'steady state' (Region III) as shown in Fig. 3(a-c). Lee and Kim have reported a reciprocating sliding friction model for the electrodeposited coatings and classified the evolution of CoF (Ref 35). During reciprocating sliding wear, the debris formed between the counter ball and the

sample is either swept away from the wear scar or piles up at the edges (Ref 36).

It is also observed in Fig. 3(a) that the CoF value decreases after certain number of cycles, which can be due to the following reasons:

1. With continuous reciprocation, the entrapped wear debris particles between the counter ball and sample surface act as a third body and the adhesive friction decreases. The abrasive friction also decreases when some amount of the wear debris is embedded in the wear scar, which reduces its roughness and due to this the attack angle of the wear debris is lowered. This may cause a reduction in the value of CoF.
2. Due to the continuous mechanical deformation the shape of the wear debris between the mating surfaces changes to spherical, which starts rolling on the surface and decreases the CoF.

At 5 and 8 N loads (in Fig. 3b and c), it is observed that the steady state is attained in a less number of cycles as compared to the 2 N load. It may be because of the high contact pressure, which wears out the top oxide layer at a faster rate. From Fig. 3(d), it is observed that the CoF value at 5 and 8 N is lower than that at 2 N load because the embedding of wear debris is more than 2 N load, which further reduces the attack angle of wear debris and decreases the abrasive friction.

Figure 4(a-c) shows the variation of CoF with the number of cycles for the single-layered Cu-SiC nanocomposite coating at

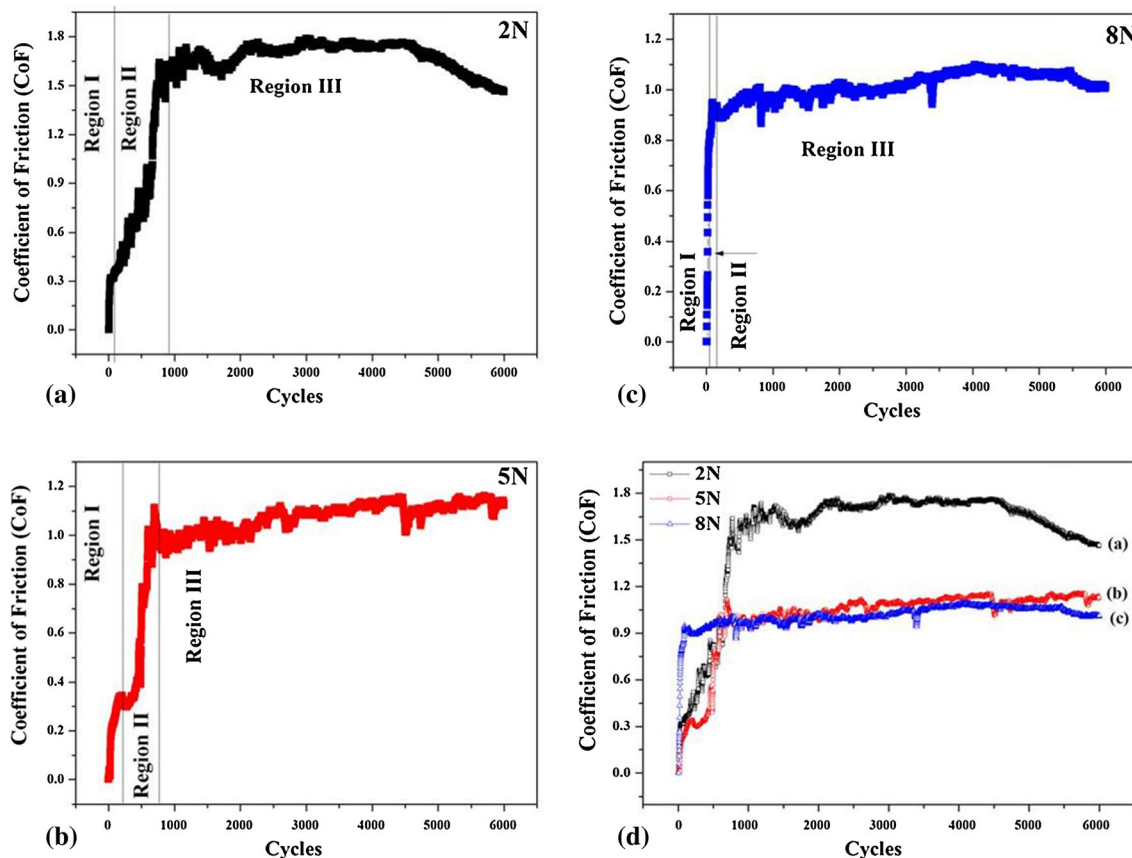


**Fig. 3** Coefficient of Friction (CoF) with number of cycles for annealed, uncoated Cu at (a) 2, (b) 5, (c) 8 N loads and (d) comparison of a, b and c

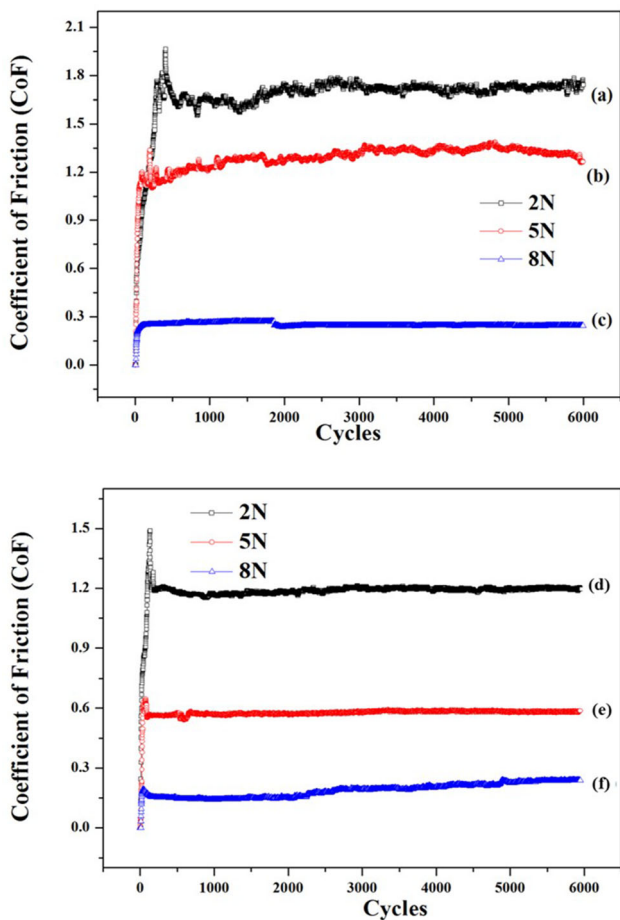


**Fig. 4** Coefficient of Friction (CoF) with number of cycles for the (a-c) single-layered Cu-SiC nanocomposite coating and (d-f) Cu, Cu-SiC FGC at (a and d) 2, (b and e) 5 and (c and f) 8N load

2, 5 and 8 N loads. Due to the presence of SiC nanoparticles, the single-layered Cu-SiC nanocomposite coating has a high hardness (3.4 GPa) and high surface roughness (1.8  $\mu\text{m}$ ) (Ref 28). Such surface tends to have a negligible adhesive contact and the CoF is produced mainly due to resistance to abrasion. The mechanical interlocking occurs between the counter ball and the asperities in the single-layered Cu-SiC nanocomposite coating, which results in a sudden rise in CoF. The CoF becomes almost constant once the asperities spall out.

From Fig. 4(d-f), it is observed that increase in load decreases the CoF, and this trend is similar to the observations in uncoated Cu and Cu-SiC nanocomposite coating on Cu. Although the top surface of the Cu, Cu-SiC FGC has 7 vol.% of uniformly dispersed SiC as in the case of single-layered Cu-SiC nanocomposite coating, the CoF is lower than the latter. The surface of Cu, Cu-SiC FGC (0.9  $\mu\text{m}$ ) is smoother than the single-layered Cu-SiC coating (Ref 28) and the soft under layers of Cu provides cushioning effect, which makes it easier for the ball to traverse on a hard surface. It is reported that the presence of graded microstructure provides cushioning effect (Ref 37).

At 2 N load (Fig. 4a and d), only the top sites of the asperities spall out from the surface. The 2 N load is not high enough to plow material and due to high surface roughness, again and again mechanical interlocking occurs resulting in high CoF. At 5 N load (Fig. 4b and e), the adhered contacting

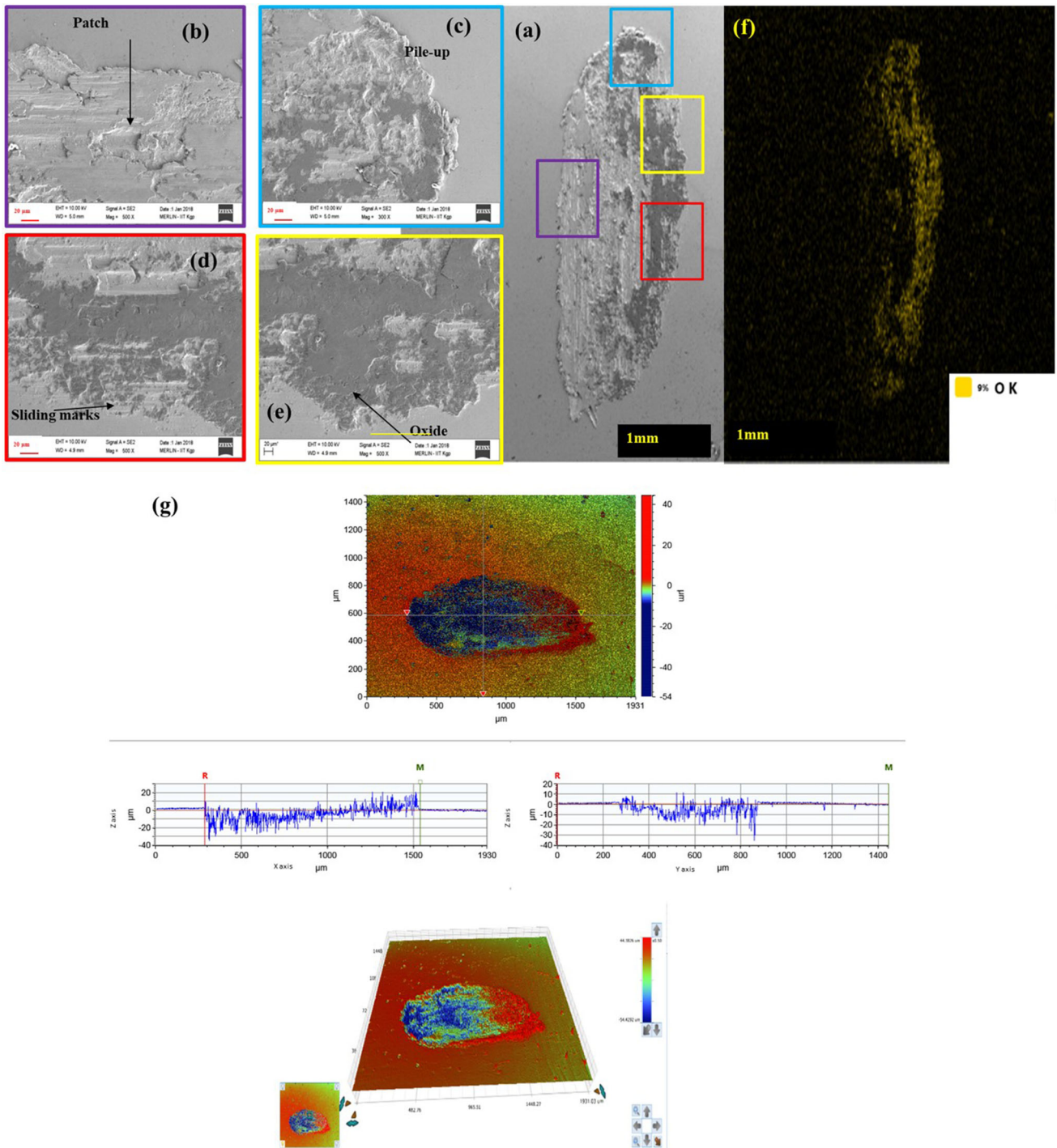
sites are sheared and the surface smoothens, which decreases the CoF value. At 8 N load (Fig. 4c and f), the surface smoothing is faster as compared to 2 and 5 N loads and after surface smoothing, there is little abrasive wear because of the high hardness of the coating.

Figure 5 shows the FESEM micrographs and the mapping of oxygen from the wear scar of annealed, uncoated Cu surface under an applied load of 2 N. Figure 5(a) shows that the wear scar is ellipsoid in shape. Figure 5(b-e) shows the magnified different regions of Fig. 5(a). Due to the plowing action, sliding marks are formed on the surface and wear debris is formed and gets accumulated around the counter ball. During reciprocation, the material at the outer edge of the ball is either thrown away from the scar or gets piled up at the edges of the scar. The material at the inner side of the ball gets embedded within the wear scar in the form of patches. The presence of oxygen shows that some of the wear debris is oxidized and embedded in the oxide form (Fig. 5f). Figure 5(g) shows the 2D and 3D surface profilometry results of the wear scar in uncoated Cu, which correlates with the FESEM micrograph in Fig. 5(a). It is observed that at 2 N load, the wear scar is shallow with a pile-up at the edges and the depth of the wear scar is due to the material loss.

Figure 6 shows the FESEM micrographs and the mapping of oxygen from the wear scar of annealed and uncoated Cu surface under an applied load of 5 N. With increase in load, the contact pressure increases, which leads to the generation, accumulation and embedding of more wear debris in the scar and it results in patches as shown from the Fig. 6(b-e), which are the magnified different regions of Fig. 6(a). The pile-up and oxide formation at the edges and patch formation in the middle areas of the wear scar are also observed. The presence of oxygen shows that some of the wear debris is oxidised and embedded in the oxide form (Fig. 6(f), corresponding to 6a). Figure 6(g) shows the 2D and 3D surface profilometry results of the wear scar in uncoated Cu, which correlates with the FESEM micrograph in Fig. 6(a). With increase in load to 5 N, the contact pressure increases, which leads to the generation, accumulation and embedding of more wear debris in the scar.

Figure 7(a) and (c) shows the FESEM micrograph and mapping of oxygen in the center of the scar from the annealed, uncoated Cu surface under an applied load of 8 N. The image (Fig. 7a) shows that the shape of the wear scar is irregular, unlike those observed in Fig. 5(a) and 6(a). The magnified image (Fig. 7b) of the edge in the wear scar shows pile-up as well as patch on the wear scar surface. It is observed from the micrographs that irregularities are present in the surface after wear due to the abrasive action of SiC particles. Plowing action at 8 N load is more compared to 2 and 5 N loads. The elemental mapping (Fig. 7c corresponding to 7a) shows that the oxide formation is present only in the center of the scar. Figure 7(d) shows the 2D and 3D optical surface profilometry results of the wear scar in uncoated Cu, which correlates with the FESEM micrograph in Fig. 7(a). It can be observed that some material is accumulated in the center of the scar.

Figure 8 shows the micrographs from the wear scar of single-layered Cu-SiC nanocomposite coating and Cu, Cu-SiC FGC at 2, 5 and 8 N loads. The image of the wear scar (Fig. 8a) shows wear at mating sites, which results in surface smoothing due to the grinding of asperity. Due to the high surface hardness of Cu-SiC nanocomposite coating, plowing action is negligible, asperities detach from the surface and the broken asperity acts as wear debris. Figure 8(b) shows that the



**Fig. 5** (a) FESEM image of the wear scar formed under an applied load of 2 N on the annealed, uncoated Cu, (b-e) magnified different regions of (a), (f) mapping of oxygen corresponding to (a) and (g) surface profilometry result of the wear scar

morphology of the wear scar at 5 N load is similar to that of the scar at 2 N load. With further increase in load to 8 N (Fig. 8c), the wear scar dimensions increase on the surface due to high abrasion by third body, i.e., wear debris. Figure 8(g), (h) and (i) show the 2D and 3D surface profilometry results of the wear scar in the single-layered Cu-SiC nanocomposite coating, which correlates with the FESEM micrograph in Fig. 8(a), (b) and (c), respectively. It can be observed that at low load, the debris gets accumulated in the rough surface of the nanocom-

posite coating. However, with increase in load, the ball plastically deforms the Cu matrix and the loose SiC nanoparticles further increase the unevenness of the coating.

Figure 8(d-f) shows the FESEM images from the wear scars of Cu, Cu-SiC FGC at 2, 5 and 8 N load. The surface hardness and roughness of Cu, Cu-SiC FGC is 3.8 GPa and 0.9  $\mu\text{m}$ , respectively (Ref 28). Although the top surface of single-layered Cu-SiC nanocomposite coating and Cu-SiC FGC is same, but CoF of the latter is less due to the smooth surface of

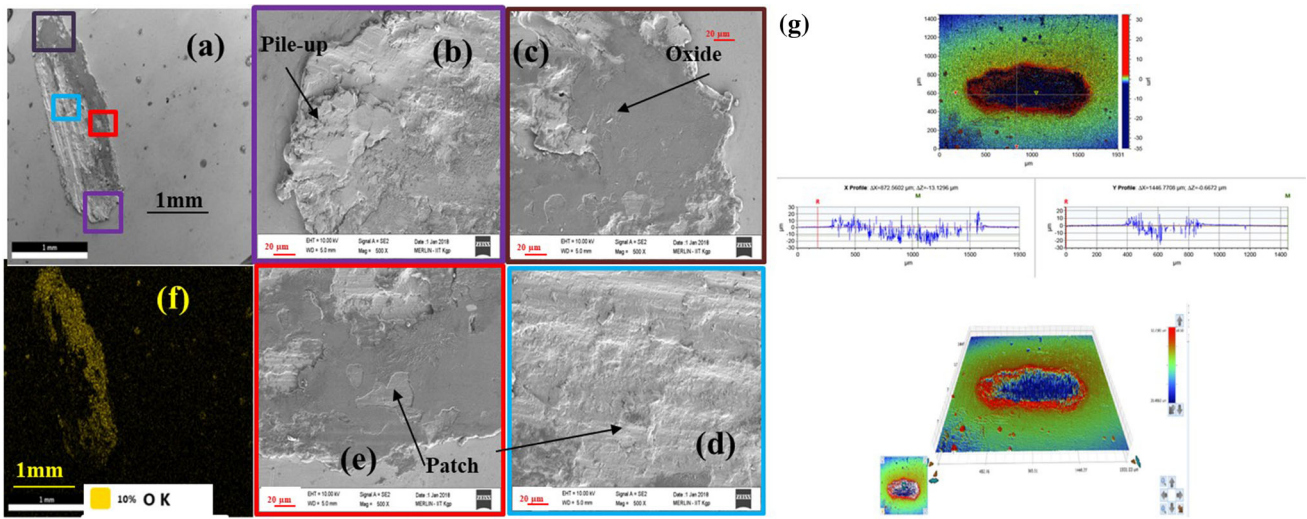


**Fig. 6** (a) FESEM image of the wear scar formed under an applied load of 5 N on the annealed, uncoated Cu, (b-e) magnified different regions of (a) and (f) mapping of oxygen corresponding to (a) and (g) surface profilometry result of the wear scar

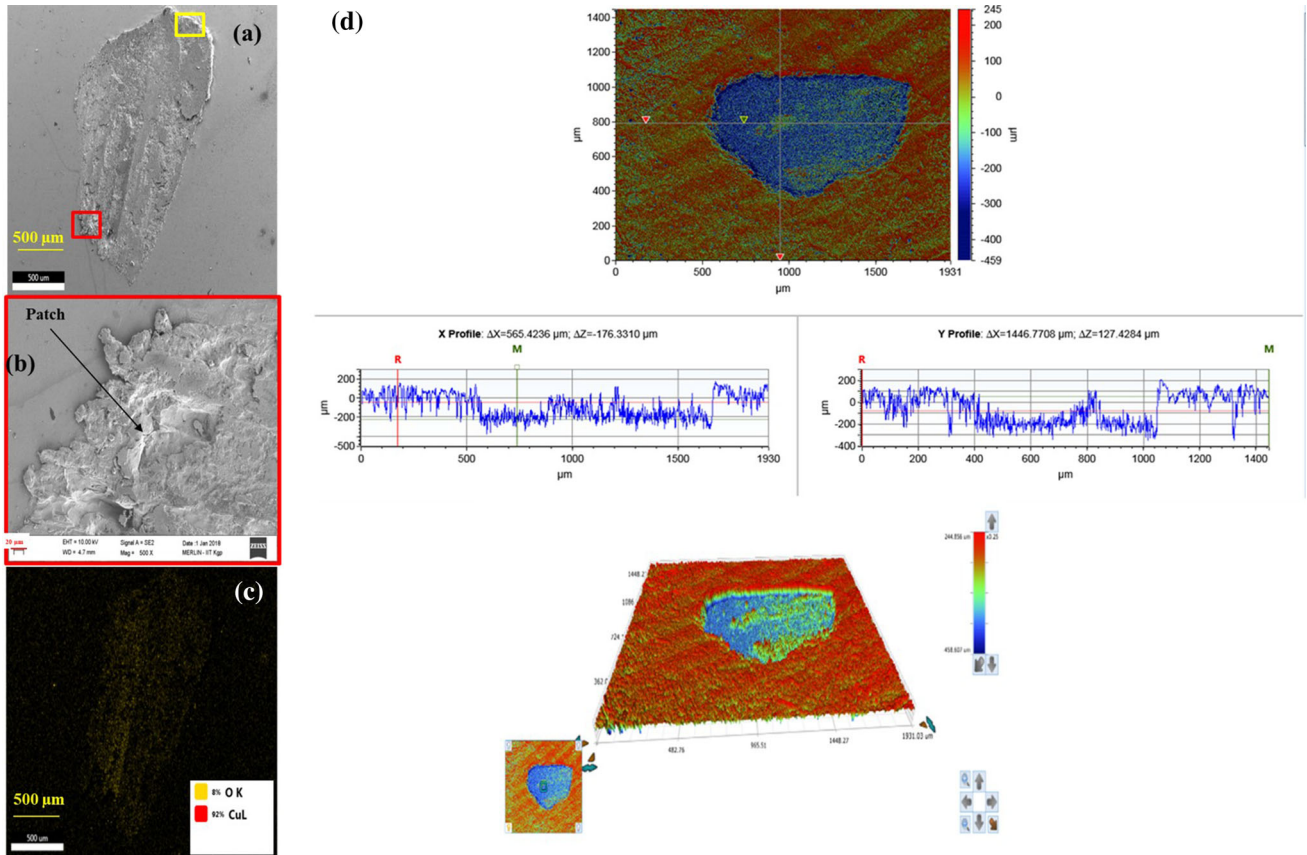


**Fig. 7** (a) FESEM images of the wear scar formed under applied load of 8 N on polished, uncoated Cu, (b) magnified different regions of (a) and (c) elemental mapping of oxygen corresponding to (a) and (d) surface profilometry result of the wear scar

Cu, Cu- SiC FGC and ductile Cu interior, which provides the cushioning effect. In the case of single-layered Cu-SiC nanocomposite coating, it is observed that the electrical resistivity is quite high (Table 1). It is due to the uniform dispersion of 7 vol.% nano-sized SiC particles in the Cu matrix throughout the 60 μm thick sample, which act as a scattering center to the path of electron flow and consequently decreases

the effective area for the current conduction and degrades the conductivity. The Cu, Cu-SiC FGC has lower resistivity than the single-layered Cu-SiC nanocomposite coating at room temperature. The volume fraction of the scattering sites in Cu, Cu-SiC FGC is less, because the SiC is restricted to the first two layers (i.e., 7 vol.% in the first 12 μm thick layer coating and 2 vol.% in the next 12 μm thick layer) of the entire coating.

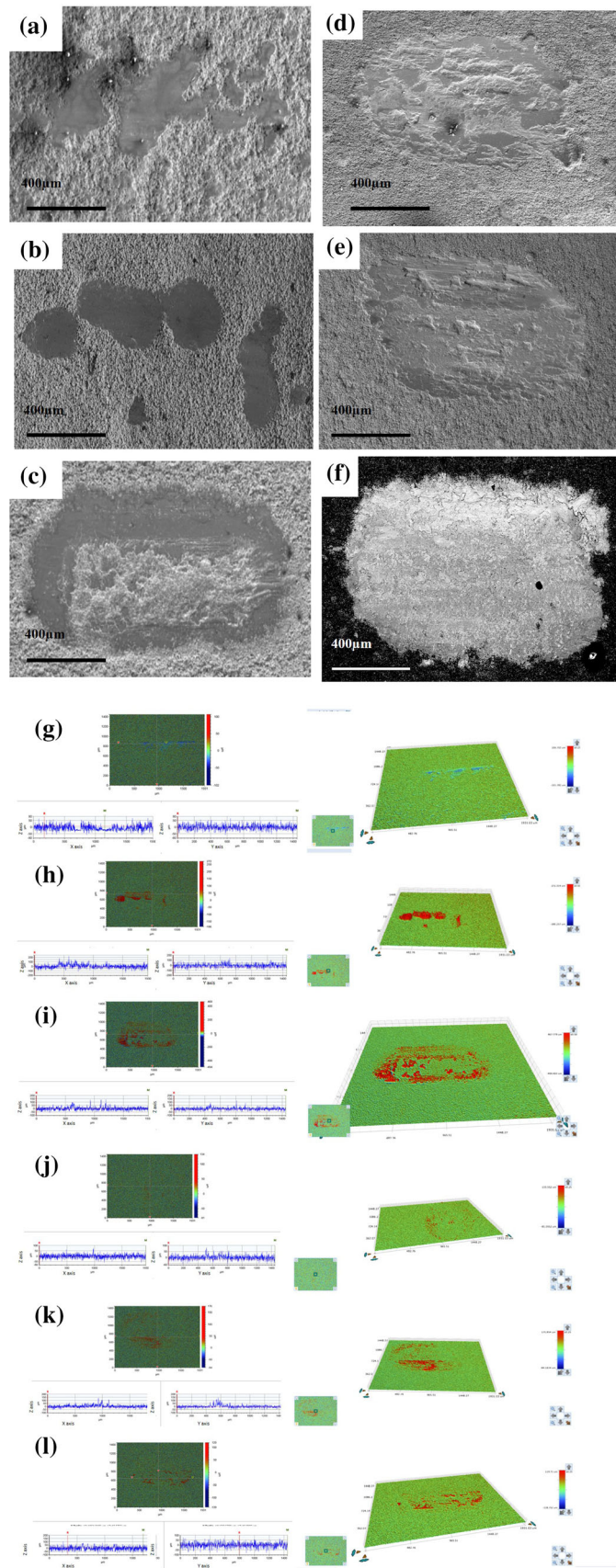


**Fig. 8** FESEM images of the (a-c) single-layered Cu-SiC nanocomposite coating and (d-f) Cu, Cu-SiC FGC at (a and d) 2, (b and e) 5, (c and f) 8 N load. Surface profilometry results of (g-i) single-layered Cu-SiC nanocomposite coating and (j-l) Cu, Cu-SiC FGC at (g and j) 2, (h and k) 5, (i and l) 8 N load



**Table 1 Electrical resistivity of Cu-SiC nanocomposite coating and Cu, Cu-SiC FGC at room temperature and comparison with the commercially available materials**

Material	Electrical resistivity, $\mu\Omega\text{cm}$	Hardness, GPa	Elastic modulus, GPa
Cu-7 vol.% SiC nanocomposite coating (present work)	$8.05 \pm 0.3$	$3.5^{27}$	$135 \pm 4$
Cu, Cu-SiC FGC (present work)	$4.71 \pm 0.1$	$3.8^{27}$	$141 \pm 3$
Cu-10% Zn <sup>8</sup>	4	0.6-1.1	125
Cu-2% Ag <sup>8</sup>	2	0.5-1.3	123
Cu-1% Cd <sup>8</sup>	3.5	0.95-1.4	124
Cu-1% Cr <sup>8</sup>	2.2	0.8-1.5	112

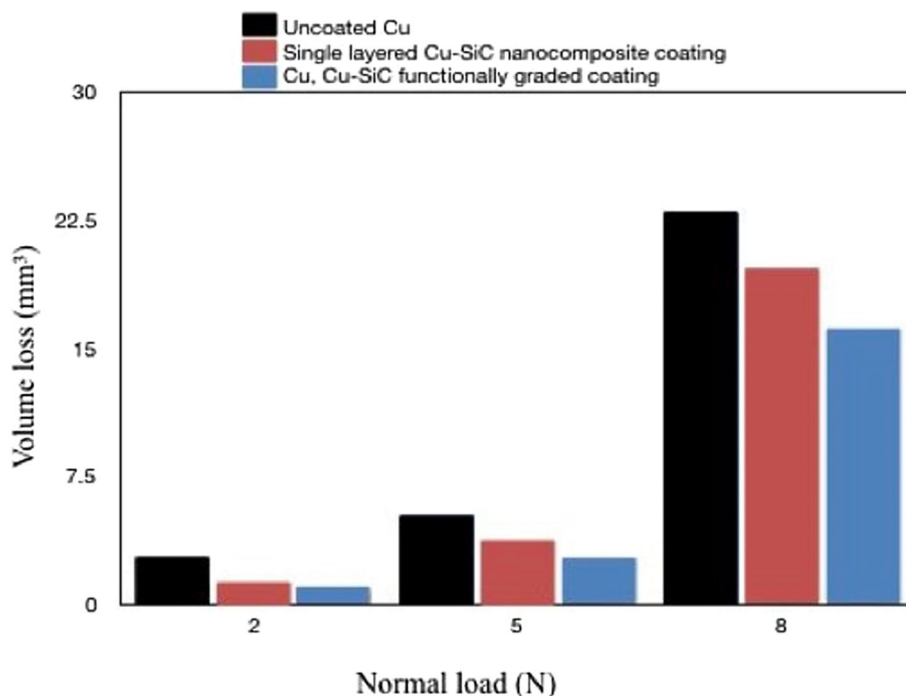
Figure 8(j), (k) and (l) show the 2D and 3D surface profilometry results of the wear scar in the single-layered Cu-SiC nanocomposite coating, which correlates with the FESEM micrograph in Fig. 8(d), (e) and (f), respectively. It can be observed that the hard SiC nanoparticles are flown away from the wear scar along with the debris and get accumulate at the edges.

Figure 9 shows the volume loss at various loads for the uncoated Cu, single-layered Cu-SiC nanocomposite coating and Cu, Cu-SiC FGC. It is observed that with increase in load, the volume loss increases in all the samples. In the uncoated Cu, the loss of material is significant with increase in load. However, in single-layered Cu-SiC nanocomposite coating and Cu, Cu-SiC FGC, the volume loss is less as compared to the uncoated sample due to the addition of hard SiC nanoparticles (Ref 27). The amount of volume loss of Cu, Cu-SiC FGC is less than single-layered Cu-SiC nanocomposite coating because of high surface roughness of the latter, which leads to high number of contact points. Thus, the total pressure exerted by counter ball is more in Cu-SiC nanocomposite coating than the Cu, Cu-SiC FGC. This results in the wearing away of surface irregularity to form a smooth surface and the debris becomes a

part of the scar by either embedding back into it or adding in the volume loss.

In the literature, it is shown that the values of electrical resistivity for the alloys (bulk material) based on Cu is in the range  $2\text{-}5 \mu\Omega\text{cm}^8$ . The measured electrical resistivity values of single-layered Cu-7vol.% SiC nanocomposite coating and Cu-Cu,SiC FGC are slightly higher than the various other alloys of Cu (Table 1). However, other properties (hardness and elastic modulus) are significantly high, which play an important role in improving the life of electrical contact. Therefore, it becomes evident that these nanocomposite coatings can be useful for various electrical applications. The thickness of these coatings is the critical parameter for determining the resistivity of the fabricated coatings. Thus, one can play with the coating thickness to reduce the values of electrical resistivity further to obtain an optimum range and the present approach provides a direction to tune the electrical properties of the nanocomposite coatings.

Figure 10 shows the ECR values measured before and after wear for all the samples. It is observed that before wear (Fig. 10a), the ECR decreases with load in all the samples because the contact area increases with increase in the contact



**Fig. 9** Volume loss vs. load of uncoated Cu, electrodeposited single-layered Cu-SiC nanocomposite coating, and Cu, Cu-SiC FGC

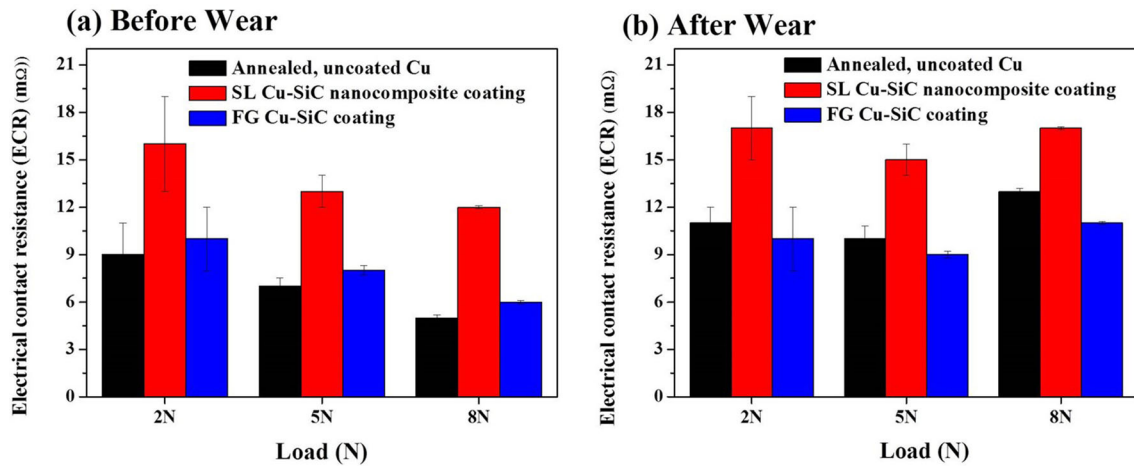


**Fig. 10** ECR of uncoated Cu, single-layered Cu-SiC nanocomposite coating and Cu, Cu-SiC FGC at room temperature (a) before and (b) after wear. The error bar shows the standard deviation

pressure. The ECR value of the uncoated annealed Cu surface is lower than the coated Cu because it is finely polished, which provides more contact sites. The ECR of single-layered Cu-SiC is more when compared to the uncoated Cu because of higher electrical resistivity and smaller real area of contact between the asperities and the counter surface. The ECR of Cu, Cu-SiC FGC is significantly lower than the single-layered Cu-SiC because of the smoother surface and lower resistivity than the latter. It is reported that the ECR depends on the resistivity, normal force, working voltage and state of contact zone (Ref 38).

The ECR values of all the samples increase after wear (Fig. 10b) because the metallic bridges are sheared away due to reciprocating sliding, which results in the formation of wear debris. This wear debris accumulated at the edges and other parts of the scar are difficult to remove from the contact area within a short period of time during traversing. With increase in load to 5 N, the ECR value decreases due to high contact pressure. On further increasing the load to 8 N, the wear debris gets embedded and seals off the contact zone and increases the ECR value in all the samples.

After wear at low load, it is observed that there is no significant change in the ECR values of single-layered Cu-SiC nanocomposite coating and Cu, Cu-SiC FGC when compared with the values before wear. At high load, there is an increment by 5 mΩ in the ECR value for both single-layered and FGC. However, the value still remains a lot less for Cu, Cu-SiC FGC than that for single-layered Cu-SiC nanocomposite coating.

## 4. Conclusions

- The value of electrical resistivity of Cu, Cu-SiC FGC is observed to be 50% less than the conventional nanocomposite coating.
- The CoF decreases with increasing applied load from 2 to 8 N in reciprocating sliding wear for all set of samples.
- The monitored value of CoF at 2 and 5 N loads is significantly less for Cu, Cu-SiC FGC than the single-layered coating and is nearly equal at 8 N load.

- At low load, the ECR values of both the coatings do not change significantly. However, at high load, this value is lot less for Cu, Cu-SiC FGC than Cu-SiC single-layered nanocomposite coating.

## Acknowledgment

The authors would like to thank Mr S. K. Karan, Technical Superintendent, Department of Physics, Indian Institute of Technology Kharagpur to help in measuring the ECR.

## Funding

The authors declare no competing financial interest.

## Compliance with Ethical Standards

## Conflict of interest

The authors declare that they have no conflict of interest.

## Human Participants and/or Animals

This work does not involve any human participants and/or animals.

## References

1. P.G. Slade, *Electrical Contacts: Principles and Applications*, second, CRC Press, Taylor & Francisgroup, 2013
2. S. Hannel, S. Fouvry, P. Kapsa, and L. Vincent, The Fretting Sliding Transition as a Criterion for Electrical Contact Performance, *Wear*, 2001, **249**, p 761–770
3. P. Jedrzejczyk, S. Fouvry, and P. Chalandon, A Fast Methodology to Quantify Electrical-Contact Behaviour Under Fretting Loading Conditions, *Wear*, 2009, **267**, p 1731–1740
4. Anon, Materials evaluation under fretting conditions, ASTM International, 1982, STP780–EB ed. WestConshohocken, PA
5. S. Fouvry and P. Kapsa, Surface damage under reciprocating sliding, *Fundamentals of Tribology and Bridging the Gap Between the Macro- and Micro/Nanoscales*, B. Bhushan, Ed., Springer, Dordrecht, 2001, p 377–391
6. G.X. Chen and Z.R. Zhou, Study on Transition Between Fretting and Reciprocating Sliding Wear, *Wear*, 2001, **250–251**, p 665–672

7. Y. Tamai, Low Friction of Metals in Reciprocating Sliding, *J. Appl. Phys.*, 1874, **1959**(32), p 1437–1440
8. D. Chapman, H.W. Turner, C. Turner, Copper in Electrical Contacts, *Copp Dev Assoc* 2015, 223
9. S. Timsit, Electrical Contact Resistance: Properties of Stationary Interfaces. in *Electrical Contacts Proceedings of the Forty-Fourth IEEE Holm Conference on Electrical Contacts* (Cat. No. 98CB36238), 1998, Arlington, VA, USA, p 1-19
10. B. Andre, *Nanocomposites for use in sliding electrical contacts*, Acta Universitatis Upsaliensis Uppsala, Sweden, 2011
11. Y. Zhan and G. Zhang, The Effect of Interfacial Modifying on the Mechanical and Wear Properties of SiCp/Cu Composites, *Mater. Lett.*, 2003, **57**, p 4583–4591
12. H. Singh, L. Kumar, S.N. Alam, Development of Cu reinforced sic particulate composites, *IOP Conf Ser Mater Sci Eng*, 2015, 75
13. R.N. Ahmed, C.S. Ramesh, Tribological properties of cast copper-SiC-Graphite hybrid composites, in *International Symposium Research Materials Science Engineering India*, 2004, p 20–22
14. G.F.C. Efe, M. Ipek, S. Zeytin, and C. Bindal, Fabrication and Properties of sic Reinforced Copper-Matrix-Composite Contact Material, *Mater. Technol.*, 2016, **50**, p 585–590
15. R. Zhang, L. Gao, Y. Pan, L. Chen, and J. Guo, Preparation of Cu/SiC FGM by Coating Method and SPS Sintering, *Mater. Sci. Forum*, 2003, **423–425**, p 249–252
16. S.G. Shiri, P. Abachi, K. Pourazarang, and M.M. Rahvard, Preparation of In Situ Cu/NbC Nanocomposite and its Functionally Graded Behavior for Electrical Contact Applications, *Trans. Nonferrous Met. Soc. China*, 2015, **25**, p 863–872
17. A. Raheem and K.A. Ali, Preparation and Mechanical Characterization of Cu-Al<sub>2</sub>O<sub>3</sub> Functionally Graded Material for Electrical Contact Applications, *J. Univ. Babylon*, 2017, **25**, p 1339–1351
18. A.K. Pradhan and S. Das, Pulse Reverse Electrodeposition of Cu-SiC Nanocomposite Coating: Effects of Surfactants and Deposition Parameters, *Metall. Mater. Trans. A*, 2014, **45**, p 5708–5720
19. A.K. Pradhan and S. Das, Pulse-Reverse Electrodeposition of Cu-SiC Nanocomposite Coating: Effect of Concentration of SiC in the Electrolyte, *J. Alloys Compd.*, 2014, **590**, p 294–302
20. S. Das, S. Banthia, A. Patra, S. Sengupta, and S.B. Singh, Novel Bilayer Zn-Ni/Ni-Co-SiC Nanocomposite Coating with Exceptional Corrosion and Wear Properties by Pulse Electrodeposition, *J. Alloys Compd.*, 2018, **738**, p 394–404
21. A. Mitra, M. Mallik, S. Sengupta, S. Banthia, S. Das, and K. Das, Effect of Anodic Passivation at High Applied Potential Difference on the Crystal Shape and Morphology of Copper Electrodeposits: Thermodynamics and Kinetics of Electrocrystallization, *Cryst. Growth Des.*, 2017, **17**(4), p 1539–1549
22. S. Banthia, S. Sengupta, M. Mallik, S. Das, and K. Das, Substrate Effect on Electrodeposited Copper Morphology and Crystal Shapes, *Surf. Eng.*, 2018, **34**, p 482–495
23. A.K. Pradhan and S. Das, Dry Sliding Wear and Friction Behavior of Cu-SiC Nanocomposite Coating Prepared by Pulse Reverse Electrodeposition, *Tribol. Trans.*, 2013, **57**, p 46–56
24. L.P.P. Chokkakula, B.V. Sarada, K.V. Rajulapati, T.N. Rao, and G. Sundararajan, A New Electrochemical Approach for the Synthesis of Copper-Graphene Nanocomposite Foils with High Hardness, *Sci. Rep.*, 2014, **4**, p 4049
25. U. Wiklund, J. Gunnars, and S. Hogmark, Influence of Residual Stresses on Fracture and Delamination of Thin Hard Coatings, *Wear*, 1999, **232**, p 262–269
26. S. Suresh, Graded Materials for Resistance to Contact Deformation and Damage, *Science*, 2001, **80**(292), p 2447–2451
27. S. Banthia, S. Sengupta, S. Das, and K. Das, Cu, Cu-SiC Functionally Graded Coating for Protection Against Corrosion and Wear, *Surf. Coat. Technol.*, 2019, **374**, p 833–844
28. S. Banthia, S. Sengupta, S. Das, and K. Das, Synthesis and Characterization of Novel Cu, Cu-SiC Functionally Graded Coating by Pulse Reverse Electrodeposition, *Appl. Surf. Sci.*, 2019, **467–468**, p 567–579
29. V. Torabinejad, M. Aliofkhaezrai, A.S. Rouhaghdam, and M.H. Allahyarzadeh, Functionally Graded Coating of Ni-Fe Fabricated by Pulse Electrodeposition, *J. Mater. Eng. Perform.*, 2016, **25**, p 5494–5501
30. M.H. Allahyarzadeh, M. Aliofkhaezrai, A.R. Sabour Rouhaghdam, and V. Torabinejad, Gradient Electrodeposition of Ni-Cu-W(alumina) Nanocomposite Coating, *Mater. Des.*, 2016, **107**, p 74–81
31. V. Torabinejad, A.S. Rouhaghdam, M. Aliofkhaezrai, and M.H. Allahyarzadeh, Ni-Fe-Al<sub>2</sub>O<sub>3</sub> Electrodeposited Nanocomposite Coating with Functionally Graded Microstructure, *Bull. Mater. Sci.*, 2016, **39**, p 857–864
32. M.H. Allahyarzadeh and M. Aliofkhaezrai, Functionally graded nickel-tungsten coating: electrodeposition, corrosion and wear behaviour, *Can. Metall. Q.*, 2016, **55**, p 303–311
33. G133-05, Linearly Reciprocating Ball-on-Flat Sliding Wear, ASTM Int, 2016, i, p 1–9
34. Standard Test Methods for Measuring Resistance of Electrical Connections Static, 2003, 02, p 1–6
35. K. Kim, J. Lee, Reciprocal sliding friction model for an electrodeposited coating and its parameter estimation using Markov Chain Monte Carlo method, *Materials* (Basel), 2016, 9
36. C.H. Hager, S. Sharma, and J.H. Sanders, Characterization of Mixed and Gross Slip Fretting Wear Regimes in Ti6Al4V Interfaces at Room Temperature, *Wear*, 2004, **257**, p 167–180
37. K. Gotlib-Vainshtein, O. Girshevit, C.N. Sukenik, D. Barlam, and S.R. Cohen, A Nanometric Cushion for Enhancing Scratch and Wear Resistance of Hard Films, *Beilstein J. Nanotechnol.*, 2014, **5**, p 1005–1015
38. X. Liu, Z. Cai, J. He, J. Peng, and M. Zhu, Effect of Elevated Temperature on Fretting Wear Under Electric Contact, *Wear*, 2017, **376–377**, p 643–665

**Publisher's Note** Springer Nature remains neutral with regard to jurisdictional claims in published maps and institutional affiliations.